HYDROCARBON SOURCE ROCKS AND GENERATION HISTORY IN THE LUNNAN OILFIELD AREA, NORTHERN TARIM BASIN (NW CHINA)

X. M. Xiao+*, Z. L. Hu* , Y B. Jin* and Z. G. Song*

In this paper we report on source rocks and maturation history at the Lunnan oilfield, northern Tarim Basin (NW China), using a combination of organic petrographic and geochemical techniques. Three separate source rock intervals are present here: Cambrian mudstones and argillaceous limestones; Middle and Upper Ordovician argillaceous limestones; and Triassic mudstones. Reservoir rocks comprise Lower Ordovician carbonates, Carboniferous sandstones, and Triassic and Jurassic sandstones. Structural traps were formed principally during the Silurian and Jurassic.

The Lunnan field is located on a small-scale palaeo uplift which developed during the Early Palaeozoic. Hydrocarbons migrated updip from source areas in surrounding palaeo-lows along faults and unconformities. Major phases of hydrocarbon generation and migration occurred in the Early Silurian – Late Devonian, Cretaceous – Early Tertiary and Late Tertiary. Uplift and intense erosion at the end of the Devonian destroyed Early Palaeozoic oil and gas accumulations sourced from the Cambrian source rocks, but hydrocarbons generated by Middle and Upper Ordovician source rocks during the Mesozoic and Tertiary have been preserved. At the present day, accumulations are characterized by a range of crude oil compositions because source rocks from different source areas with different maturation histories are involved.

INTRODUCTION

The *Lunnan* field is located in the centre of the Tabei Uplift in the northern Tarim Basin, NW China (Fig. 1), in a region referred to as the Lunnan "Low Uplift" or "Lunnan area" by Chinese geologists. The field is characterized by multiple reservoir intervals which produce crude oils with a range of physical properties (Hanson *et al.,* 2000; Huang, 1994; Huang, 1998; Huang, 2000; Liang *et al.*, 1998; Liang, 1999). Reservoir rocks consist of Ordovician carbonates, Carboniferous sandstones, and Triassic and Jurassic sandstones. Crude oil types include normal oils, heavy oils and light oils with variable wax contents (Hanson *et al.*, 2000; Liang *et al.*, 1998). There has been considerable research on the origin of the oil and gas in this area in the past few years (Gu *et al.*, 1999; Hanson *et al.*, 2000; Huang, 1998; Jia, 1999; Liu, 1991; Liu and Chen, 1991; Kang, 1992; Tong, 1991; Zhuo *et al.*, 1997; Zhang *et al.*, 2000), but much of this research has focused either on regional geology or on geochemistry. In the present study, we combine geological and geochemical methods to investigate the origin of oil and gas in the *Lunnan* area. Particular attention is paid to the relationship between source rocks, hydrocarbon-generation histories, reservoir and cap rocks, and the evolution of trap structures.

*State Key Laboratory of Organic Geochemistry, Guangzhou Institute of Geochemistry, Chinese Academy of Sciences, Guangzhou 510640, P R China.
+author for correspondence, email: xmxiao@gig.ac.cn

Geological setting and sample locations

The Early Palaeozoic Lunnan Uplift separates the Early Palaeozoic Chuhu Depression to the east from the Mesozoic Halahatang Depression to the west (Fig.1). To the south is the Early Palaeozoic Manjiaer Depression. The uplift is bounded to the north by the roughly east-west trending Luntai (or Shaya-Luntai) Fault which marked the northern boundary of the Tarim Basin throughout much of the Palaeozoic. The Lunnan Uplift can be divided into a number of structural units – the Lunnan and Satamu fault belts and the Jilaki-Jifanchudong anticline (Fig.1) – each of which hosts a number of oil - and gasfields.

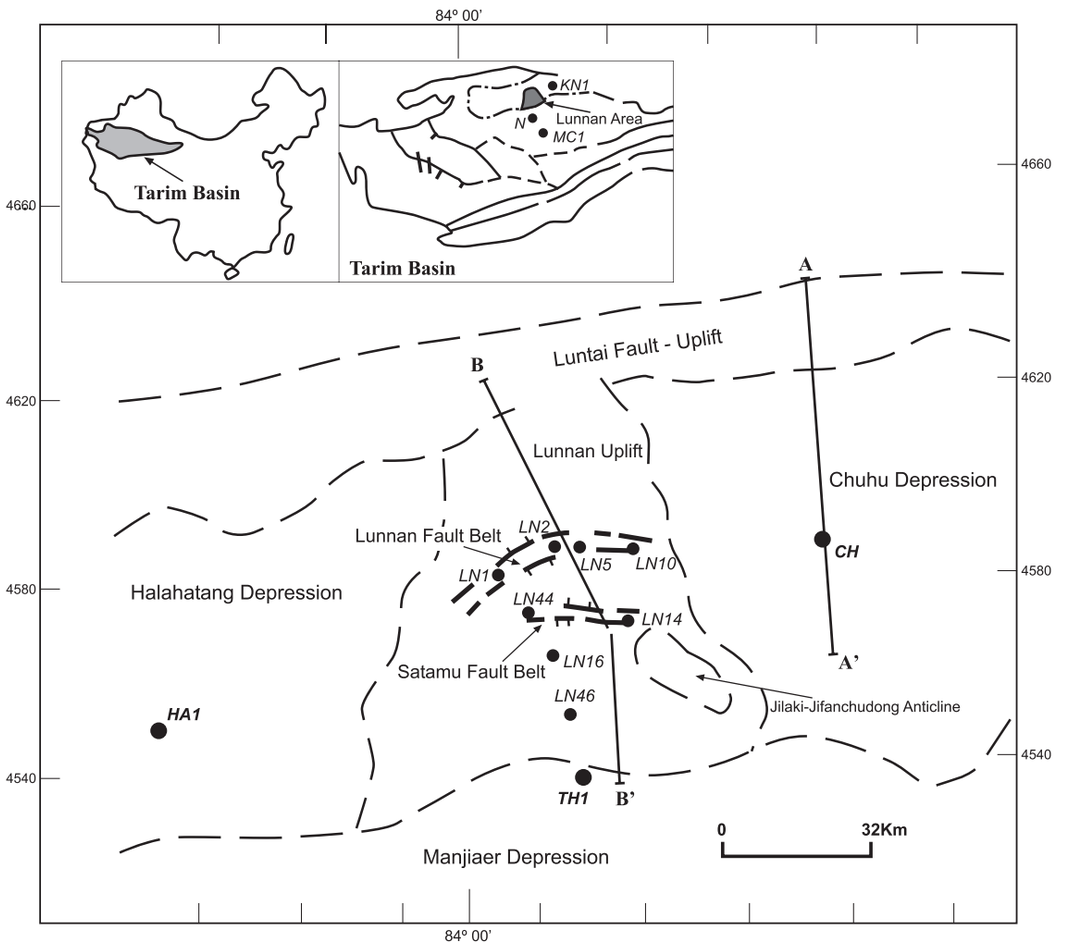

Fig.1. Structural sketch map of the *Lunnan* area, northern Tarim Basin, with the locations of the wells studied (map after Wang and Li, 1993). Profiles A-A' and B-B' are shown in Fig. 2.

The stratigraphic column in the *Lunnan* area includes Early Palaeozoic, Late Palaeozoic, Mesozoic and Cenozoic strata with a total thickness of 7,000 - 9,000m (Fong *et al.*, 1991; Liang and Wang 1991; Duan *et al.*, 1998; Jia, 1999) (Figs.2 and 3). Middle and Upper Ordovician - Devonian strata are absent over most of the area as a result of intense Silurian-Devonian uplift and erosion (Kang, 1992; Huang, 1998). Reservoirs with commercial volumes of oil and gas are present in Ordovician carbonates and Carboniferous, Triassic and Jurassic sandstones (Hanson *et al.*, 2000; Huang, 1998; Zhuo *et al.*, 1997, Zhang *et al.*, 2000). Oil-prone source rock occur in the Lower and Middle Cambrian and Middle and Upper Ordovician successions in the Manjiaer and Chuhu Depressions (Hanson *et al.*, 2000; Liang *et al.*, 1998; Zhang *et al.*, 2000). Triassic strata in the *Lunnan* area also have source-rock potential (Xiao, 1997).

MATERIALS AND METHODS

Around 100 mudstone and argillaceous limestone core samples with source rock potential were recovered from wells in and around *Lunnan* field (locations are shown in Fig.1). A *Rock-Eval III* instrument was used for pyrolysis analysis of whole rock samples. An *MPV III* microphotometer was used for reflectance measurements and microscopic observations. Kerogens for maceral analysis were isolated from source rocks following the methods outlind by Alpern (1980). In most cases, whole rock polished blocks were used for reflectance measurements. In samples where it was difficult to find sufficient macerals for reflectance measurements, or where it was necessary to measure micrinite reflectance, polished kerogen samples were used. For rocks of Late Palaeozoic and Mesozoic ages, vitrinite reflectance was used as an index of maturity. However, for Early Palaeozoic samples which lack vitrinite, the reflectance of vitrinite-like macerals, bitumen and micrinite was assessed for maturity evaluation (Xiao, 1992; Xiao *et al.*, 1991). A larger measured field was set up during microscopy in order to minimize the influence of the optical textures of the bitumen or the micrinite on the measured reflectance results. Data were discounted if there were less than 15

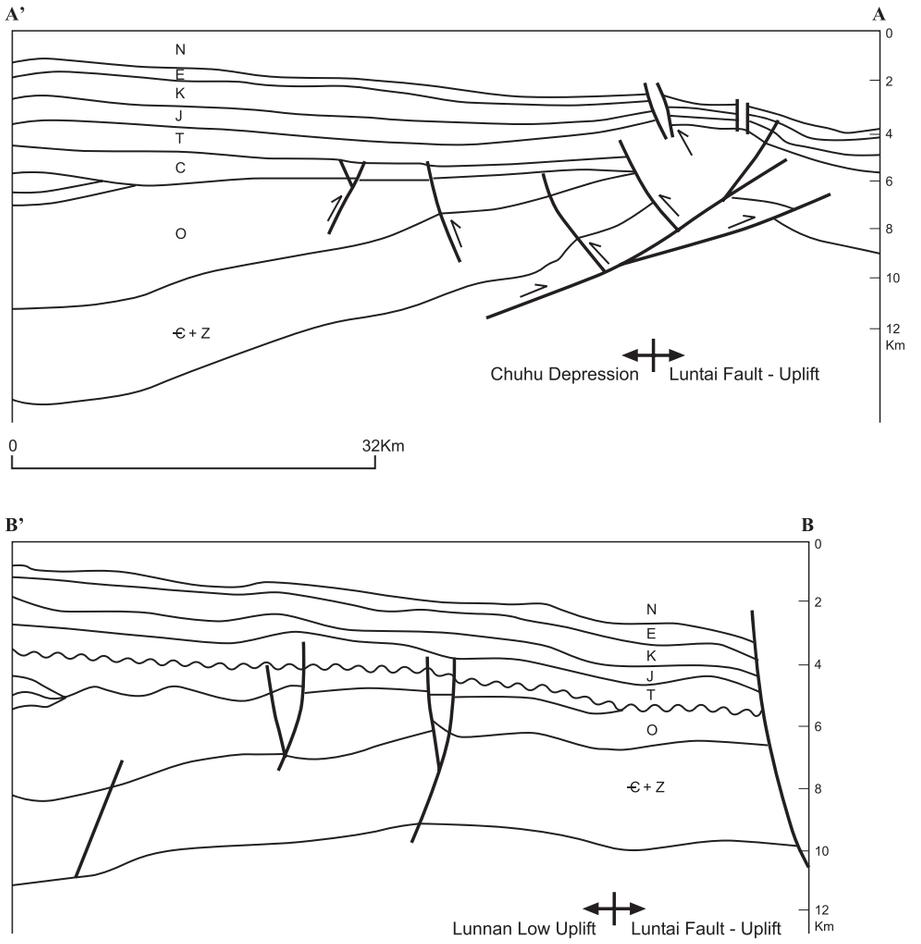

Fig.2. Interpreted seismic sections through the *Lunnan* area. Profile locations are marked on Fig. 1 (after Wang and Li, 1993).

measurements on each type of maceral per sample, or if the standard deviation for the reflectance was greater than 0.1% (Ro <1.0%) and 0.15% (Ro = 1.0-2.0%).

Measured reflectance values of bitumen, micrinite and vitrinite-like macerals, abbreviated as %BRo, %MRo and %VLMRo, respectively, were calibrated to equivalent vitrinite reflectance (% VRo) using the following equations:

VRo% = 0.668 BRo +0.346 (Liu and Shi, 1994);

VRo% = 1.26 VLMRo + 0.21 (VLMRo < 0.75%) (Xiao *et al.*, 2000c);

VRo% = 0.28 VLMRo + 1.03 (VLMRo = 0.75 - 1.50%) (Xiao *et al.*, 2000c);

VRo% = 0.81 VLMRo + 0.18 (VLMRo >1.50%) (Xiao *et al.*, 2000c);

VRo% = 0.75 MRo + 0.51 (Xiao *et al.*, 1991).

RESULTS AND DISCUSSION

Source rock evaluation

Triassic mudstones

Triassic mudstones in the *Lunnan* area are 100-300m thick (Huang, 1994; Jin, 1997; Liang, 1992; Xiao, 1997). TOC is generally 0.80 - 1.50%, and Rock-Eval HI is 100-250 mg/g (Table 1); vitrinite reflectance ranges from 0.60-0.80%.

The results of maceral analysis indicated that biodegraded amorphinite or micrinite was the main constituent in around half of the samples, with a content of 30-60% (Table 2). Biodegraded amorphinite is derived from biodegradation of organic material of variable origin. Xiao *et al.* (1998) divided it into three submacerals, referred to as biodegraded amorphinite A, B and C, whose hydrocarbon potentials approximate to those of kerogen Types I, IIa and IIb, respectively. Micrinite is the thermal degradation product of biodegraded amorphinite after the main stage of oil generation. It also can be subdivided into corresponding submacerals, referred to as Micrinite A, B and C (Xiao *et al.*, 1998). Biodegraded

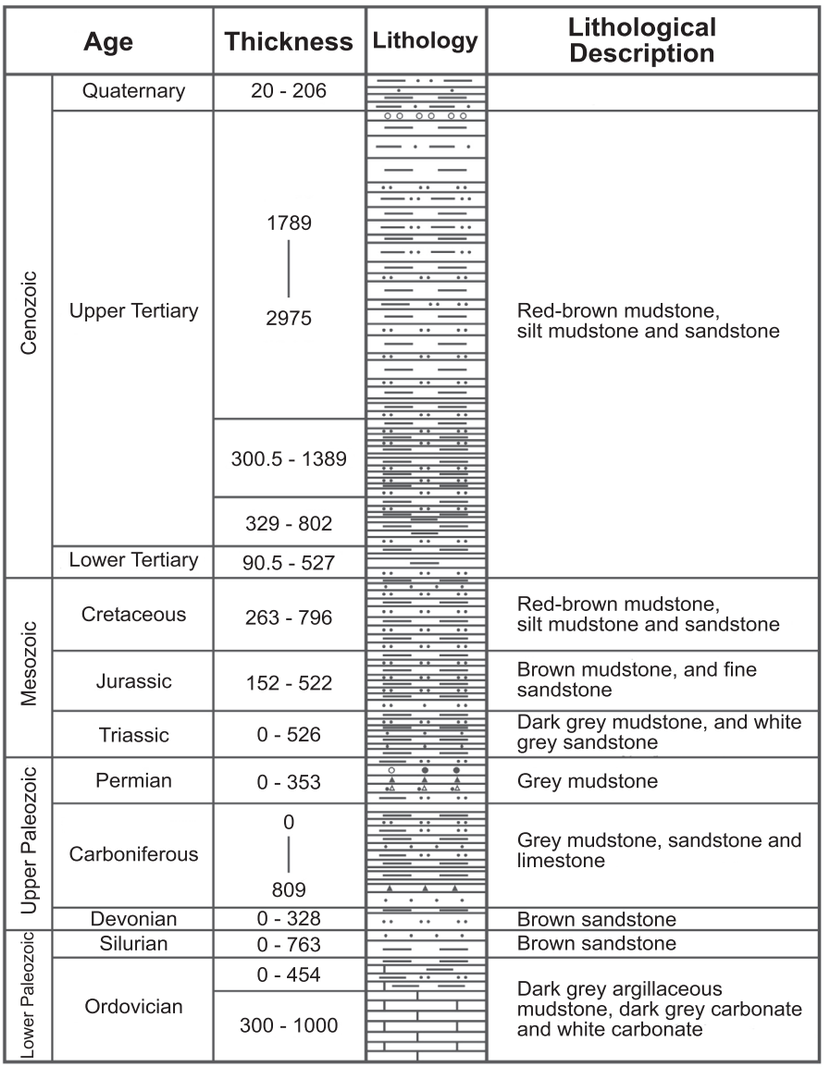

Fig.3. Stratigraphy of the *Lunnan* area (modified after Wang and Li, 1993).

amorphinite generates oil much earlier than other macerals under equivalent conditions, with the oil window ranging from 0.40 to 0.85% VRo (Xiao, 1992). According to Xiao (1997), Triassic source rocks show a suppression of vitrinite reflectance by 0.1-0.15% VRo. Therefore, most Triassic source rocks in this area are mature. In some samples, microscopic observations indicated that the biodegraded amorphinite was altered into micrinite after it had generated oil; Triassic mudstones can therefore be classified as significant source rocks in the *Lunnan* area. The oil generated may have migrated into Triassic and Jurassic reservoir sandstones.

Carboniferous mudstones

Carboniferous mudstones are 100-150 m thick in the *Lunnan* area (Liang and Wang, 1991). TOC generally ranges from 0.50-1.0% and vitrinite reflectance is in the range 0.70-0.90%. The kerogen consists mainly of vitrinite and inertinite, and Rock-Eval HI is generally < 80 mg/g (kerogen Types III or IV: Tables 3 and 4). The mudstones are interpreted to have little or no oil potential.

Middle and Upper Ordovician argillaceous limestones

Argillaceous limestones of Middle and Late Ordovician ages are 20-50 m thick in the southern part of the *Lunnan* area (Liang *et al.*, 1998; Liu and Wen 1998), and seismic data indicate that they may reach over 100m in thickness in the Manjiaer Depression (Liang, 1999; Liang *et al.*, 1998). Samples from well *LN46* had TOCs of 0.2-0.9% and were mature with an equivalent VRo of 1.0-1.35%. The organic matter was Type II (Table 5 and 6). These data suggest that the Ordovician argillaceous limestones may constitute a fair source rock, as defined by Peters and Gassa (1994), and have

Well	Depth (m)	Age	Lithology	TOC (wt %)	S1(mg/g)	S2(mg/g)	Tmax (°C)	HI (mg/g)
LN1	4646.5	J	Dark grey mudstone	0.76	0.04	0.74	438	97
LN1	4815	T	Black grey mudstone	1.38	0.03	2.76	440	200
LN1	4825	T	Black/ grey mudstone	1.68	0.25	4.12	437	280
LN1	4883	T	Black/ grey mudstone	1.97	0.39	4.96	439	241
LN1	4941	T	Dark grey mudstone	0.56	0.06	0.78	437	139
LN1	5039	T	Dark grey mudstone	0.7	0.01	0.33	441	47
LN1	5042	T	Dark grey mudstone	1.02	0.04	0.58	446	57
LN10	4397	J	Grey mustone	0.21	0.02	0.07	400	33
LN10	4638	T	Black/ grey silty mudstone	1.54	0.3	2.45	440	159
LN10	4692	T	Dark grey mudstone	0.79	0.05	0.91	432	115
LN10	4897	T	Dark grey mudstone	0.32	0.03	0.38	438	118
LN10	5023	T	Dark grey mudstone	0.68	0.05	0.43	427	63
LN10	5113	T	Dark grey mudstone	0.71	0.06	0.21	455	30
LN16	4259	J	Dark grey mudstone	0.97	0.02	1.03	434	106
LN16	4529	T	Black grey mudstone	0.56	0.01	0.33	433	59
LN16	4590	T	Grey black mudstone	1.44	0.03	1.21	34	84
LN26-1	4846	T	Grey mudstone	0.62	0.04	0.6	442	96
LN26-1	4849	T	Grey mudstone	0.54	0.02	0.59	438	109
LN26-1	5013	T	Dark grey mudstone	1.36	0.12	1.08	440	29
LN46	4187	T	Dark grey mudstone	0.9	0.02	1.82	434	202
LN46	4190	T	Dark grey mudstone	1.02	0.18	1.98	439	194
LN46	4192	T	Black mudstone	7.14	0.93	17.75	433	248
LN46	4354	T	Dark grey mudstone	1.09	0.08	0.97	443	45
LC2	5662	T	Black/ grey mudstone	0.57	0.12	0.16	431	45
LC2	5665	T	Black/ grey mudstone	0.81	0.01	0.25	440	31
LC2	5919	T	Black /grey mudstone	1.06	0.06	0.48	440	45
HA1	4770	T	Black /grey mudstone	1	0.11	0.09	437	9
HA1	4802	T	Dark grey mudstone	2.17	0.09	4.27	434	197
HA1	5137	T	Black/ grey mudstone	4.92	0.13	9.13	433	186
HA1	5223	T	Black/ grey mudstone	2.34	0.07	1.98	439	85
MC1	2782	J	Dark gray mudstone	0.45	0.02	0.06	429	13
MC1	2812	T	Dark grey mudstone	0.38	0.03	0.12	421	32
MC1	2825	T	Dark grey mudstone	0.36	0.03	0.12	421	33
MC1	3138	T	Black grey mudstone	0.54	0.03	0.58	433	107
MC1	3591	T	Black grey mudstone	0.54	0.03	0.59	441	109

Table 1. TOC and Rock-Eval analytical results for Triassic (T) and Jurassic (J) mudstones from wells in the *Lunnan* area. Well locations in Fig. 1.

generated a significant amount of oil, consistent with oil-source rock correlation studies (Liang *et al.*, 1998).

Cambrian shales and argillaceous limestones

Cambrian strata have not been penetrated by the drill in the *Lunnan* area. Seismic data indicate that they are about 50-200m thick in the Manjiaer and Chuhu Depressions (Liang *et al.*, 1998; Liu and Wen, 1998; Yung and Liu, 1991). Well *KN1*, located in the Tabei Uplift to the east of *Lunnan* (Fig.1), penetrated Cambrian black shales and dark argillaceous limestones which were about 60m thick. Samples from this well were analyzed for their hydrocarbon potential (Tables 5 and 6). TOC was 1.5-2.3%, and equivalent VRo was 1.8-2.0%. Although the HI was quite low as a result of their very high maturation levels, the dominant maceral was micrinite, indicating that their original organic matter was Types I and II (Xiao, 1992). This suggests that they were orignally good source rocks which may have generated significant volumes of hydrocarbons.

Source rock maturation history

The three source rock intervals identified in the *Lunnan* area – Lower and Middle Cambrian shales and argillaceous limestones; Middle and Upper Ordovician argillaceous limestones; and Triassic mudstones – have had different burial and maturation histories. Fig.4a illustrates the burial history of well *LN46* in the southern *Lunnan* area, while Fig.4b illustrates that of well *MC1* in the Manjiaer Depression. The plots show that the burial history of the Early Palaeozoic interval at these two locations is very different. The burial history at well *LN46* can be divided into three stages:

(i) Stage I (Cambrian to Early Devonian): Around 4,000-4,500m of sediments were deposited during this

Well	Depth(m)	Age	Lithology	VRo(%)	Maceral analysis of kerogen (%)							Kerogen
					V	I	E	A	Amor(C)	Ha	M(C)	type
LN1	4646.5	J	Dark grey mudstone	0.53	21.3	10.8	28.5	0	40.4	0	0	IIb
LN1	4815	T	Black grey mudstone	0.55	9.7	11	14	0	65.3	0	0	IIb
LN1	4825	T	Black grey mudstone	0.44	6.5	1.2	19.5	0.5	72.3	0	0	IIb
LN1	4883	T	Black grey mudstone	0.72	24.3	4.2	13.2	0	58.3	0	0	IIb
LN1	4941	T	Dark grey mudstone	0.74	36.8	15.4	16.8	0	31	0	0	IIb
LN1	5039	T	Dark grey mudstone	0.84	45.8	12	4	0	0	38.2	0	III
LN1	5042	T	Dark grey mudstone	0.76	26	11	2.3	0	0	0	67	IIb
LN10	4397	J	Grey mudstone	0.6	44.5	44.8	10.7	0	0	0	0	III
LN10	4638	T	Black grey silty mudstone	0.49	12.3	5	26.3	0	56.36	0	0	IIb
LN10	4692	T	Dark grey mudstone	0.63	4.5	10.3	4.5	0	0	45.6	0	III
LN10	4897	T	Dark grey mudstone	0.7	30.6	38.6	6.8	0	0	24	0	III
LN10	5023	T	Dark grey mudstone	0.74	14.5	6.9	0	0	0	0	79	IIb
LN16	4259	J	Dark grey mudstone	0.66	80	5	15	0	0	0	0	III
LN16	4529	T	Black grey mudstone	0.61	48.7	41.2	10.2	0	0	0	0	III
LN16	4590	T	Black gray mudstone	0.67	79	12.7	8.3	0	0	0	0	III
LN26-1	4846	T	Grey mudstone	0.58	21.5	41.5	13	0.5	0	23.5	0	III
LN26-1	4849	T	Grey mudstone	0.61	74.3	23.1	2.6	0	0	0	0	III
LN26-1	5013	T	Dark grey mudstone	0.72	62.3	18.9	3	0	0	15.8	0	III
LN46	4187	T	Dark grey mudstone	0.6	14.6	3.4	16	0	65*	0	0	IIb
LN46	4190	T	Dark grey mudstone	0.59	38.8	2.6	58.6	0	0	0	0	III
LN46	4192	T	Black mudstone	0.58	34.1	5.9	10	0	50	0	0	IIb
LN46	4354	T	Dark grey mudstone	0.62	78.8	16	15.4	0	0	0	0	III
LC2	5662	T	Black gray mudstone	0.89	26.5	10	0.5	0	0	0	63	IIb
LC2	5665	T	Black grey mudstone	0.84	24.3	18	1.08	0	0	0	56.6	IIb
LC2	5919	T	Black grey mudstone	0.96	17.8	6.9	0	0	0	0	75.3	IIb
HA1	4770	T	Black grey mudstone	0.6	25.3	73.7	1	0	0	0	0	III
HA1	4802	T	Dark grey mudstone	0.65	24.3	4	8.1	0	0	0	63.7	IIb
HA1	5137	T	Black grey mudstone	0.65	18.3	3.4	6.9	0	0	0	71.4	IIb
HA1	5223	T	Black grey mudstone	0.74	69.2	20.8	11.01	0	0	0	0	III
MC1	2782	J	Dark grey mudstone	0.53	17.8	69.35	12.9	0	0	0	0	IV
MC1	2825	T	Dark grey mudstone	0.57	19.8	78.4	1.8	0	0	0	0	IV

Table 2. Measured vitrinite reflectance and maceral analysis results for kerogens derived from Triassic (T) and Jurassic (J) mudstones. Well locations in Fig. 1. V: vitrinite; I, inertinite; E, exinite; A, alginite; Amor, biodegraded amorphinite B; Ha, humic amorphinite; M(B), micrinite B; * biodegraded amorphinite C.

Well	Depth(m)	Age	Lithology	TOC(%)	S1(mg/g)	S2(mg/g)	Tmax(°C)	HI(mg/g)
LN10	5023	C	Dark grey mudstone	0.68	0.15	0.43	446	63
LN15	5230	C	Dark grey mudstone	0.6	0.3	0.28	434	47
LN16	4849	C	Dark grey silty mudstone	0.71	0.25	0.52	442	73
LN16	4919	C	Black grey mudstone	1.03	0.1	0.48	429	47
LN16	5131	C	Dark grey mudstone	0.43	0.11	0.38	448	88
LN16	5373	C	Grey mudstone	0.15	0.08	0.1	436	67
LN16	5581	C	Dark grey mudstone	0.43	0.21	0.2	440	47
LN32	5430	C	Dark grey mudstone	0.16	0.13	0.02	/	12
LN32	4684	C	Black mudstone	0.82	0.12	0.42	432	39
LN32	4769	C	Grey mudstone	0.2	0.01	0	/	0
LN32	5352	C	Dark grey mudstone	0.4	0.1	0.19	427	48
TH1	4846	C	Gray silt mudstone	0.08	0.01	0.01	/	13
TH1	4969	C	Dark grey mudstone	0.12	0.01	0.01	436	8
TH1	5028	C	Dark grey mudstone	0.15	0.12	0.02	/	13
TH1	5158	C	Dark grey mudstone	0.16	0.01	0.04	426	25
TH1	5417	C	Dark grey mudstone	0.17	0.01	0.05	441	29
JN1	5246	C	Grey silt mudstone	0.06	0	0.1	432	17
C2	5213	C	Black mudstone	0.44	0.11	0.25	440	57
C2	5277	C	Dark grey mudstone	0.21	0.08	0.18	439	86
C2	5298	C	Dark grey silt mudstone	0.68	0.13	0.44	441	65
C2	5434	C	Dark grey mudstone	0.72	0.09	0.59	439	69
MC1	3560	P	Dark grey mudstone	0.4	0.06	0.1	427	25
MC1	4254	C	Dark grey mudstone	0.71	0.41	0.75	442	105
MC1	4765	C	Dark grey argillaceous lmstn	1.92	0.54	3.57	428	185

Table 3. TOC and Rock-Eval analytical results for Carboniferous (C) and Permian (P) mudstones from wells in the *Lunnan* area. Well locations in Fig. 1

time interval which was terminated by a phase of intense uplift and erosion in the Late Devonian associated with the late Caledonian orogeny.

(ii) Stage II (Carboniferous to Early Tertiary): During this stage, the burial history of well *LN46* was significantly different to that at well *MC1*. The *Lunnan* well location underwent slow subsidence with very little or no maturation of source rocks. However, source rock maturation was continuous at the *MC1* location throughout this stage.

(iii) Stage III (Late Tertiary): The *Lunnan* area subsided rapidly with the deposition of some 3,000 m of sediments, leading to rapid thermal maturation of source rocks.

Palaeotemperature gradients

Palaeotemperature gradients in the Tarim Basin have recently been studied by Jin (1997), Xiao *et al.* (2000b) and Xiao *et al.* (2001). In general, palaeotemperature gradients in the basin have been fairly low throughout its history. Previous studies have shown that gradients in the *Lunnan* area were around 2-3°C/100m, while those in the Manjiaer Depression were slightly lower, about 1.8-2.3°C/100m (Jin, 1997; Xiao *et al.*, 2000b; and Xiao *et al.*, 2001). We took average gradients to be 2.5°C/100m and 2.0°C/100m, respectively. The palaeo- surface temperature in this area was taken to be 20°C (Jin, 1997; Liang *et al.*, 1998).

THERMAL MATURATION MODELLING

Palaeozoic Source Rocks

The *Lunnan* area is characterized by alternating periods of uplift and subsidence (Fig. 4). Previous studies have shown that the TTI method is not suitable for a basin with this kind of history (Jin, 1997; Xiao *et al.*, 2000b). Xiao *et al.* (2000b) described a modified version of Karweil's method to model the thermal maturation of source rocks in the Tarim Basin and obtained reasonable results. In this method, the palaeotemperature gradient and palaeo-surface temperature is combined with burial history to model VRo evolution. This method was used in the present study for four different areas (Fig.1): the Chuhu Depression; the Southern Tabei Uplift (between wells *LN46* and *TH1*); the northern Manjaer Depression (some 60 km south of well *TH1* at location "N" in Fig.1); and the central Manjiaer Depression.

(i) The Chuhu Depression (Fig. 5)

The modelled location ("Ch" in Fig.1) is in the centre of the Chuhu Depression. The oil window and main stage of oil generation for Cambrian

Well	Depth(m)	Age	Lithology	VRo(%)	Maceral analysis of kerogen (%)					Kerogen
					V	VIM	I	E	M(C)	type
LN15	5230	C	Dark grey mudstone	0.76	18.9	0.5	6.4	2.5	71.7	IIb
LN16	4849	C	Dark grey mudstone	0.73	26.5	0.5	2	0.5	0	III
LN16	4919	C	Black grey mudsrone	0.79	50.4	0.5	29.6	19.6	0	III
LN16	5131	C	Dark grey mudstone	0.78	71.9	1.8	6.8	20.5	0	III
LN16	5373	C	Grey mudstone	0.75	58.2	0.5	16.8	24.5	0	III
LN16	5581	C	Dark grey mudstone	0.8	64.3	0.5	18.9	16.3	0	III
LN32	5430	C	Dark grey mudstone	0.83	91	0	8.5	0.5	0	III
LN32	4684	C	Black mudstone	0.71	64.5	0	29	6.5	0	III
LN32	4769	C	Grey mudstone	0.74	13.2	0	85.3	1.5	0	IV
LN32	5352	C	Dark gray mudstone	0.89	58.9	0	39.1	0.5	0	III
TH1	4846	C	Grey silty mudstone	0.67	34	9	64	1	0	IV
TH1	4969	C	Dark grey mudstone	0.85	33.2	0	64.3	2.5	0	IV
TH1	5028	C	Dark grey mudstone	0.81	55.5	0	43	1.5	0	III
TH1	5158	C	Dark grey silty mudstone	0.86	2	0	0.5	0	97.5	IIb
TH1	5417	C	Dark grey silty mudstone	0.95	71.2	0.5	24.3	3.5	0	III
JN1	5246	C	Dark grey silty mudstone	1.02	80	2.5	16.5	1	0	III
C2	5213	C	Black mudstone	0.63	56.4	6.8	29.8	6.8	0	III
C2	5277	C	Grey mudstone	0.73	65.3	1.8	26	6.9	0	III
C2	5298	C	Dark grey silty mudstone	0.8	64.2	0.5	31.5	3.8	0	III
C2	5434	C	Dark grey mudstone	0.84	80	0	16.5	3.5	0	III
MC1	3509	P	Dark grey mudstone	0.61	68.9	0	28.8	2.3	0	III
MC1	4254	C	Dark grey mudstone	0.71	64.3	5.2	14.1	16.4	0	III
MC1	4765	C	Dark grey argillaceous limestone	0.78	11.3	6.8	4.5	11.8	65.6*	IIb

Table 4. Measured vitrinite reflectance and maceral analysis results for kerogens derived from Carboniferous and Permian mudstones. V: vitrinite;VIM, vitrinite-like macerals; I, inertinite; E, exinite; M, micrinite B; * biodegraded amorphinite.

Well	Depth(m)	Age	Lithology	TOC(%)	S1(mg/g)	S2(mg/g)	Tmax(℃)	HI(mg/g)
LN46	5569	O2-3	Dark grey argillaceous limestone	0.19	0.1	0.08	449	42
LN46	5759	O2-3	Dark grey argillaceous limestone	0.21	0.04	0.02	447	10
LN46	5667	O2-3	Dark grey argillaceous limestone	0.2	0.05	0.02	446	10
LN46	5835	O2-3	Dark grey argillaceous limestone	0.24	0	0.05	444	20
LN46	6076	O2-3	Dark grey argillaceous limestone	0.1	0.12	0.08	437	80
LN46	6155	O2-3	Dark grey argillaceous limestone	0.19	0.83	0.06	436	32
LN46	6106	O2-3	Dark grey argillaceous limestone	0.15	0.3	0.05	435	33
LN10	5229	O1	Grey limestone	0.1	0.1	0.1	/	10
LN10	5390	O1	Grey limestone	0.12	0.15	0.1	452	83
LN10	5482	O1	Grey limestone	0.11	9.12	0.09	448	81
LN10	5600	O1	Grey limestone	0.14	0.08	0.09	450	64
LN10	5689	O1	Grey limestone	0.1	0.06	0	/	0
LN10	5801	O1	Grey limestone	0.09	0.25	0.66	448	66
KN1	5189	∈1-2	Black argillaceous limestone	0.24	0	0	/	0
KN1	5192	∈1-2	Black argillaceous limestone	0.98	0.18	0.1	424	10
KN1	5199	∈1-2	Black argillaceous limestone	1.03	0.1	0.1	442	9
KN1	5503	∈1-2	Black argillaceous limestone	1.67	0.08	0.08	442	5
KN1	5506	∈1-2	Black argillaceous limestone	2.01	0.03	0.04	/	2
KN1	5508	∈1-2	Black argillaceous limestone	2.24	0.01	0	/	0

Table 5. TOC and Rock-Eval analytical results for Cambrian-Ordovician mudstones and argillaceous limestones from wells in the *Lunnan* area (well locations in Fig. 1).

source rocks occurred here at 450-220Ma and 400-230Ma, respectively. The oil window and main stage of oil generation for Ordovician source rocks occurred at 380-100Ma and 380-100Ma, respectively (Fig.5).

(ii) The South Tabei Uplift (Fig. 6)

The modelled location was well *LN46*. Here, the oil window and main stage of oil generation for Cambrian source rocks occurred at 410-210Ma and 280-230Ma, respectively; and for Ordovician source rocks at 225-5Ma and 130-15 Ma, respectively (Fig.6).

(iii) The Northern Manjiaer Depression (Fig.7)

At location "N" (Fig.1), the oil window and main stage of oil generation for Cambrian source rocks occurred at 430-390Ma and 400-380Ma, respectively; and for Ordovician source rocks, at 390-125Ma and 300-225 Ma, respectively (Fig.7).

(iv) The central Manjiaer Depression (Fig.8)

At the *MC1* well location in the centre of the Depression, the oil window and main stage of oil generation for Cambrian source rocks occurred at 460-415Ma and 445-425Ma, respectively; and for Ordovician source rocks at 425-350Ma and 400-380Ma, respectively (Fig.8).

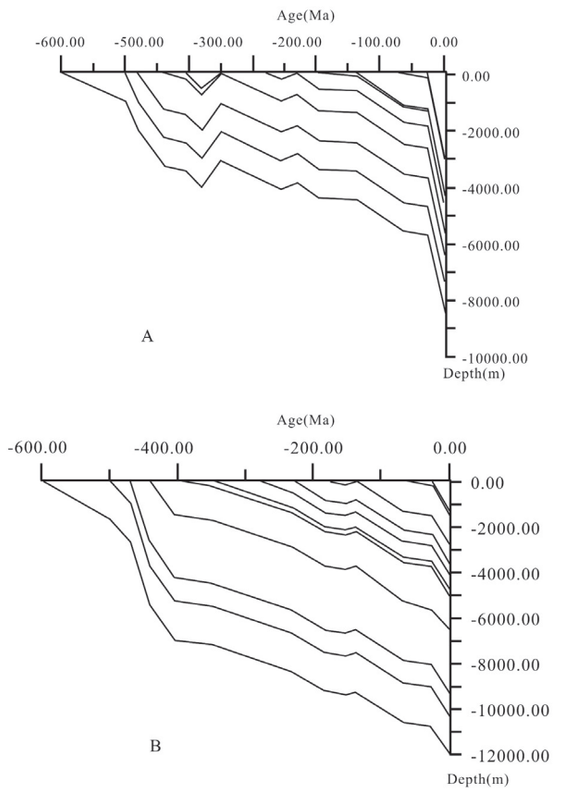

Fig.4. Burial histories for wells (a) *LN46* and (b) *MC1* (locations in Fig.1). Note the differences in the burial history of the Early Palaeozoic strata between the two well locations. Data from Wang and Li (1993).

Triassic Source Rocks

Vitrinite reflectance profiles for Triassic source rocks at three well locations in the Lunnan area are presented in Fig.9. VRo values for samples from a single well increase with their present-day burial depths. The

Well	Depth(m)	Age	Lithology	Maceral analysis of kerogen (%)					Kerogen
				VLM	ILM	A	M(A) or M(B)	B	type
LN46	5569	O2-3	Dark grey argillaceous lmstn	3	2	0.2	90.6(B)	4.1	IIa
LM46	5759	O2-3	Dark grey argillaceous lmstn	2.8	0	5.5	89.5(B)	1	IIa
LN46	5667	O2-3	Dark grey argillaceous lmstn	4.9	9.8	2.5	75.6(B)	7.3	IIa
LN46	5835	O2-3	Dark grey argillaceous lmstn	14.5	22.9	0.84	52.6(B)	9.2	IIa
LN46	6076	O2-3	Dark grey argillaceous lmstn	3.8	17.9	0	78.3(B)	0	IIa
LN46	6155	O2-3	Dark grey argillaceous lmstn	4.6	19.5	0	75.9(B)	0	IIa
LN10	5229	O1	Grey mudstone	0	1	0	98(B)	1	IIa
LN10	5390	O1	Grey mudstone	0	0	0	100(B)	0	IIa
LN10	5482	O1	Grey mudstone	0	3.4	0	96(B)	0.6	IIa
LN10	5600	O1	Grey mudstone	0	0	0	98(B)	2	IIa
LN10	5689	O1	Grey mudstone	0	0	0	100(B)	0	IIa
LN10	5801	O1	Grey mudstone	0	0	0	100(B)	0	IIa
KN1	5189	∈1-2	Black argillaceous lmstn	0	1	0	96(A)	3	I
KN1	5192	∈1-2	Black argillaceous lmstn	0	1	0	97(A)	2	I
KN1	5199	∈1-2	Black argillaceous lmstn	0	0	0	98(A)	2	I
KN1	5503	∈1-2	Black argillaceous lmstn	0	0	0	95(A)	5	I
KN1	5506	∈1-2	Black argillaceous lmstn	0	0	2	97(A)	1	I
KN1	5508	∈1-2	Black argillaceous lmstn	0	3.5	0	96(A)	0.5	I

Table 6. Maceral analysis results for kerogens derived from Cambrian-Ordovician argillaceous limestones. VIM, vitrinite-like maceral ; ILM, inertinite-like maceral; A, alginite; M(B), micrinite B; M(A), micrinite A; B, bitumen.

burial history at wells *LN46* and *MC1* (Fig.4) indicate that the Triassic strata had a burial depth of 1,900-2,300 m with a temperature of 64-66°C at the end of the Early Tertiary, and are currently buried to 4,200-5,300 m with a temperature of 117-126°C. This implies that the Triassic source rocks entered the main stage of oil generation in the Late Tertiary.

Discussion

Oil generation in the *Lunnan* area occurred between the Silurian and the Tertiary. Three peaks in hydrocarbon generation can be identified: Early Silurian–Early Devonian; Cretaceous-Early Tertiary; and Late Tertiary. The amount to which each phase has contributed to present-day hydrocarbon accumulations in the *Lunnan* area depends on timing and the relationships between reservoir and cap rocks, traps, and regional tectonism.

Four reservoir-cap rock couplets have been recognized in the *Lunnan* area: Ordovician carbonates and argillaceous limestones; Carboniferous sandstones and mudstones; Triassic sandstones and mudstones; and Jurassic sandstones and mudstones (Duan *et al.*, 1998; Fong et al, 1991; Liu, 1991). Reservoir and cap rocks of Early Palaeozoic age were destroyed as a result of uplift and erosion during the Late Devonian. However, Early Silurian tar sandstones have been recorded in well *HA1*; and Early Ordovician carbonates stained with bitumen in wells *LN14* and

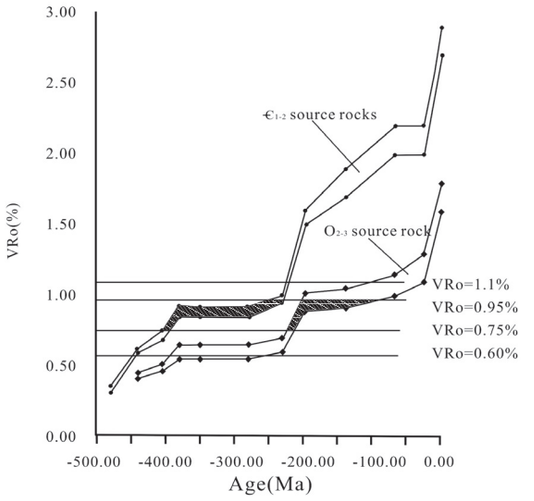

Fig.5. Hydrocarbon-generating histories for Early Palaeozoic source rocks in the Chuhu Depression. The oil window and peak stage for oil generation are confined to VRo in the range of 0.60%-1.10% and 0.75%-0.95%, respectively.

Organic inclusion group	Organic inclusions			Homog. temp*	Bitumen group	Type of associated bitumen	
	Fluorescence properties	Size(um)	Liquid/gas ratio			Bitumen reflectance (%)	Optical properties
Group I	Yellow, yellow green	3 to 6	Pure liquid hydrocarbon	80-90	Group I	1.1-1.35	Optical anisotropy, mosaic texture
Group II	Green yellow	2 to 15	90:10-80:20	60-70	Group II	0.8-1.0	Very weak optical anisotropy, homogeneous texture,
Group III	Green, blue green	1 to 3	80:20-60:40	100-150	Group II	<0.05	Yellow-brown fluorescence

Table 7. Characteristics of bitumen and organic inclusions in Ordovician strata in the *Lunnan* area.

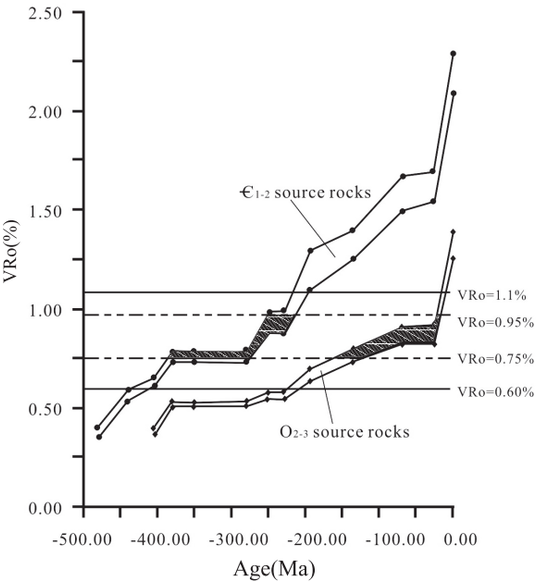

Fig.6. Hydrocarbon-generation histories of source rocks in well *LN46*, South Tabei Uplift. The oil window and peak stage for oil generation is defined in Fig.5.

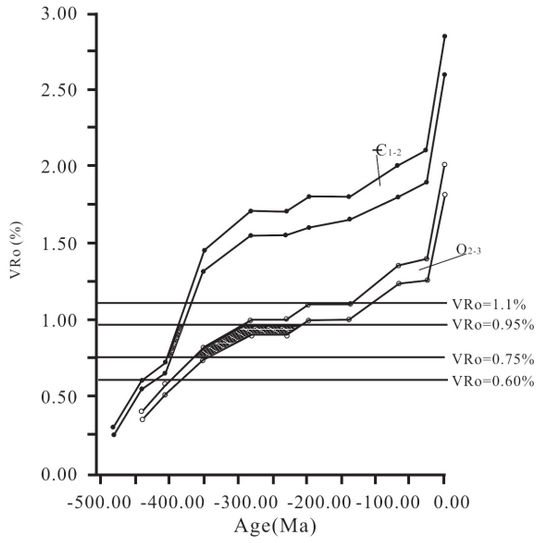

Fig. 7. Hydrocarbon-generating histories of source rocks in the northern Manjiaer Depression. The oil window and peak stage for oil generation is defined in Fig.5.

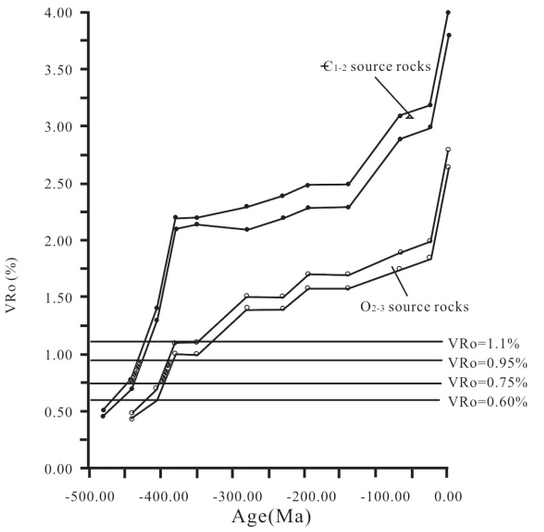

Fig.8. Hydrocarbon-generating histories for source rocks in well *MC1*, central Manjiaer Depression.

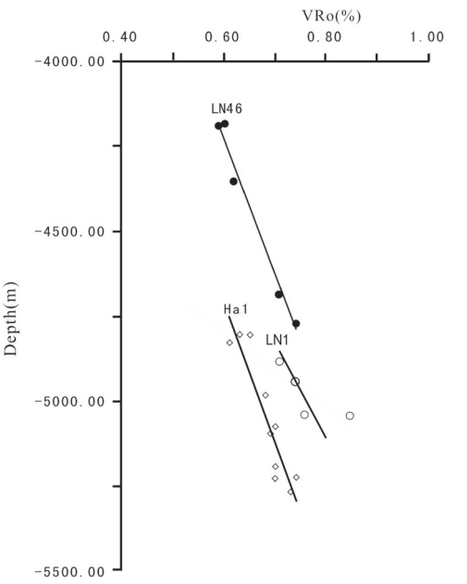

Fig.9. Relationship between vitrinite reflectance values and depth for Triassic source rocks at three well locations in the *Lunnan* area.

JF126 provide further evidence for the existence of palaeo- oil and gas pools in this area (Liu, 1997; Zhang *et al.*, 2003; Hanson *et al.*, 2003).

The Silurian and the Jurassic were the most important periods for trap formation. The Tabei Uplift was formed during the Silurian resulting in the formation of Early Palaeozoic structural traps (Duan *et al.*, 1998; Tang, 1997; Tang *et al.*, 1991). In the Jurassic, the Xunshan orogenic phase resulted in the formation of structures involving Late Palaeozoic and Mesozoic strata (Liu and Chen, 1991; Zhuo *et al.*, 1997; Zhou *et al.*, 1991).

Anticlines are the main type of structural trap in the *Lunnan* area, and most commercial oil and gas pools occur in anticlinal folds or associated fault zones (Duan *et al.*, 1998; Zhuo *et al.*, 1997). Fault zones provided migration pathways into reservoir rocks (Fig.10).

PETROLEUM MIGRATION

Three types of bitumen inclusions have been identified in Lower Paleozoic rocks in the *Lunnan* area (Table 7) and provide direct evidence for petroleum generation and migration. Since bitumen reflectance values provide an indication of the thermal maturation history of solid bitumens after their emplacement in the reservoir rock or carrier unit, it is possible to deduce the time when the bitumen accumulated by combining reflectance measurements with the inferred burial and palaeotemperature histories of the host sediments. Thus Xiao *et al.* (2000a) modelled the timing of bitumen accumulation in the *Lunnan* area using this method. They proposed that the first phase of bitumen accumulation occurred during the Early Devonian, the second phase during the Cretaceous-Early Tertiary, and the third phase during the Late Tertiary. These three phases of bitumen accumulation are comparable to the main stages of petroleum generation estimated from our source rock maturation studies.This suggests that there have been three episodes of large-scale petroleum generation and migration in the Lunnan area.

Since the Lunnan Uplift began to develop in the Early Palaeozoic (Tong, 1991; Tang, 1997; Liu, 1991), petroleum has migrated updip towards it from surrounding source kitchens (Fig.10). Migration pathways include faults and unconformity surfaces. Faults cut through the Palaeozoic succession and provide pathways for the migration of petroleum from upper and middle Ordovician source rocks into younger reservoir units, and also result in the mixing of petroleum from different sources. This geological background suggests that petroleum from Triassic source rocks has mainly migrated into the Mesozoic reservoir rocks.

PETROLEUM EVENTS IN THE LUNNAN AREA

As described above, there are three potential source rock intervals in the *Lunnan* area, with separate phases of petroleum migration and accumulation. Three petroleum "events" can be recognized in the area:

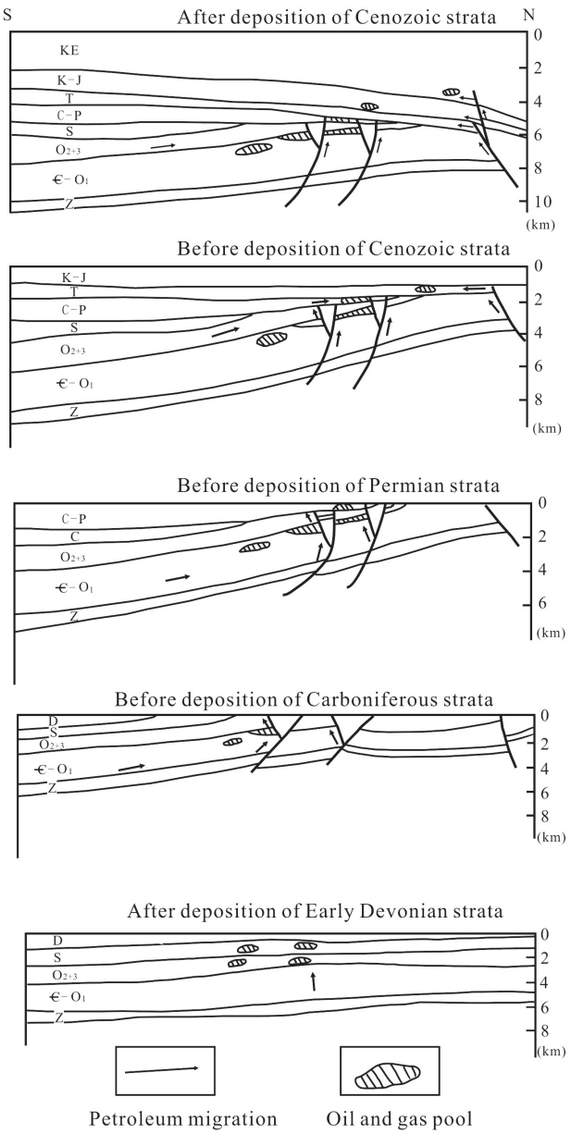

Fig.10. Cartoons showing petroleum migration pathways and the evolution of oil and gas pools in the *Lunnan* area during the Late Devonian - Tertiary.

1. Early Palaeozoic: This event involved source rocks of Cambrian age in the centre of the Manjiaer and Chuhu Depressions. The main stage of oil generation occurred during the Middle Silurian to Early Devonian. The Tabei Uplift formed during the Silurian. Oil and gas migrated along faults and unconformity surfaces into Early Ordovician carbonates and Lower Silurian sandstones. Intense uplift occurred in this area during the Late Devonian and the reservoirs were breached or destroyed.

The occurrences of tar sandstones in Lower Silurian strata in the Tabei area (Liu, 1997), and of carbonates containing bitumen in a number of wells in the Lunnan area (Xiao *et al.*, 2001) provide direct evidence for the existence of palaeo-oil and gas accumulations.

2. Cretaceous – Early Tertiary: This event involved Middle and Upper Ordovician argillaceous limestone source rocks which occur in the northern margin of the Manjiaer Depression and the western margin of the Chuhu Depression. The main stage of oil generation occurred during the Cretaceous - Early Tertiary, and petroleum migrated into reservoirs of various different ages. Since this petroleum event persisted for a long period of time and involved source rocks with a wide range of maturation levels, the resulting petroleum has a variety of physical properties. This event made a significant contribution to the oil and gas pools in the *Lunnan* area.

3. Late Tertiary: This event involved Middle and Upper Ordovician argillaceous limestones in the

southern part of the Lunnan area and Triassic mudstones elsewhere; in consequence, two types of oils were formed. The oil and gas generated by Middle and Upper Ordovician source rocks migrated into reservoir rocks of various ages along faults and unconformity surfaces. However, petroleum from Triassic source rocks mainly migrated into Mesozoic reservoirs. Petroleum formed during this event not only accumulated in individual trap structures, but more often entered previously formed reservoirs. This complicated generation history may explain why there are so many different types of crude oil in the *Lunnan* field reservoirs.

CONCLUSIONS

The geological and geochemical conditions accompanying the formation of oil and gas pools in the *Lunnan* area are complex. Several sets of source rocks are present within the Silurian-Tertiary interval. They occur in different areas and have quite different hydrocarbon-generating histories. A number of reservoir-cap rock combinations developed, with ages from Ordovician to Jurassic.Structural traps -- simple and faulted anticlines -- generally formed during the Silurian and Jurassic. Regional faults and unconformity surfaces provided channels for petroleum migration.

Three petroleum generation events are recognized in the *Lunnan* area: Early Palaeozoic, Cretaceous - Early Tertiary; and Late Tertiary. The oil and gas pools formed during the Early Palaeozoic were destroyed during uplift and erosion in the Late Devonian. The occurrence of tar sandstones in Lower Silurian strata and of bitumen in Lower Ordovician carbonates is evidence for the existence of palaeo-oil and gas pools. The later two petroleum events contributed to the formation of the present-day oil and gas accumulations.They involved different source rocks from different areas with quite different maturation histories, and the resulting oil and gas has mixed in the reservoir. Thus, individual oil and gas pools in this area have a complex origin and are characterized by the co-existence of different types of crude oil.

ACKNOWLEDGEMENTS

The authors are indebted to A. D. Hanson for improving the English and for constructive comments and suggestions on the original manuscript. The assistance of JPG editorial staff with the English language presentation is also acknowledged.This paper arises from Chinese Academy of Sciences Project GIGCX-04-08. It was also supported by Chinese State 973 projects (Granted No.2003CB214607 and contract G199043308).

REFERENCES

ALPERN, B., 1980. The Petrology of Kerogen. In: Durand, B. (Ed.), Kerogen. Editions Technip, (Paris), pp.284-321.

DUAN, T. J., XU, H. J. and WU, H.,1998. Trapping structures related to faults in the Tarim Basin. *Experimental Petroleum Geology*, **20**(7), 217-222 (in Chinese).

FONG, Q.,ZHOU, D.Z., and WANG, G. ,1991. Tectonic features and their control on oil and gas pools in the Tabei Uplift. In: Tang, X. G. and Liang, D. G. (Eds), Paper Compilation of Oil and Gas Formation in the Tarim Basin. Xinjiang Science and Sanitation Press (Wulumuqi), pp. 267-277(in Chinese).

GU, Q.Y., PAN, W.Q. and CHAO, S.Z., 1999. Characteristics of oil and gas pools in Ordovician strata in the Lunnan Area. *Xinjiang Petroleum Geology* **20**(3), 210-212 (in Chinese).

HANSON, A. D., ZHANG, S. C., MOLDOWAN, J. M., *et al.*, 2000. Molecular organic geochemistry of the Tarim basin, northwest China. *AAPG Bull.* **84**(8), 1109-1128.

HUANG, D. F., 1994. Geochemical characteristics of source rocks in the Tarim Basin. Internal report. Beijing Institute of Petroleum Exploration and Development, pp.149-189 (in Chinese).

HUANG, C.B., 1998. Formation and distribution of oil and gas pools in the Taibei Uplift of the Tarim Basin. *Xinjiang Petroleum Geology*, **19**(5), 357-361(in Chinese).

HUANG, C.B., 2000. Geological conditions to form oil and gas pools in Cambrian - Ordovician strata in the Tarim Basin. *Xinjiang Petroleum Geology* **21**(3),188-192(in Chinese).

JIA, C. Z., 1999. Structural characteristics and petroleum accumulation in Tarim Basin. *Xinjiang Petroleum Geology*, **20**(3), 177-183 (in Chinese).

JIN, K.L. (Ed.), 1997. Organic Petrology: a Case Study of the Tarim Basin. Seismic Press, Beijing, pp155-180 (in Chinese).

KANG, Y. Z., 1992. Oil and gas fields of Palaeozoic age in the Tarim Basin. China University of Geoscience Press, (Beijing), pp.51-71 (in Chinese).

LIANG, D. G., 1999. Several geological problems of oil and gas exploration in the Tarim Basin. *Xinjiang Petroleum Geology*, **20**(3), 184-188 (in Chinese).

LIANG, D. G. AND WANG, F. C. ,1991. Petroleum sources in the Tarim Basin. In: Tang, X. G. and Liang, D. G. (Ed.), Paper Compilation of Oil and Gas Formation in the Tarim Basin. Xinjiang Science and Sanitation Press, (Wulumuqi), pp.321-330 (in Chinese).

LIANG, D. G., ZHANG, S.C. and WANG, F.Y., 1998. Study on source rocks and oil sources in the Tarim Baisn. Internal Report. Beijing Institute of Petroleum Exploration and Development, pp.32-124 (in Chinese).

LIU, D. M. ,1991. Tectonic evolution and its effect on the formation of oil and gas pools in the Lunnan Area. In: Tang, X. G. and Liang, D. G. (Eds), Paper Compilation of Oil and Gas Formation in the Tarim Basin. Xinjiang Science and Sanitation Press, (Wulumuqi), pp. 274-279 (in Chinese).

LIU, N. F. ,1997. The origin of bitumen sandstone in Tarim Basin. Internal Report. Petroleum University, (Beijing), pp. 26-57 (in Chinese).

LIU, C.Y. and CHEN, H.W., 1991. The petroleum geological characteristics and distribution pattern of oil and gas pools of Triassic strata in the Lunnan Area, Tarim Basin. In: Tang, X. G. and Liang, D. G. (Eds), Paper Compilation of Oil and Gas Formation in the Tarim Basin. Xinjiang Science and Sanitation Press, (Wulumuqi), pp. 497-504 (in Chinese).

LIU, H, and WEN, D., 1998. The distribution and evaluation of the Early Palaeozoic source rocks in the Manjiaer Depression. Internal Report. Tarim Petroleum Geology Institute. (Kuerlia, Xinjiang), pp. 1-32 (in Chinese).

PETERS, K.E. and CASSA, M.R., 1994. Applied source rock

geochemistry. In: L.B. Magoon and W.G. Dow, (Eds), The Petroleum System—From Source to Trap. *AAPG Mem.* **60**, 93–117.

TANG, L. J., 1997. A preliminary investigation of the tectonic movements in the Tarim Basin. *Experimental Petroleum Geology* **19**(2), 108-121(in Chinese)

TANG, H.S., GUO, G.H. and ZHOU, L., 1991. Origin of trapping structures and types of oil and gas pools in Ordovician strata in the Lunnan Area of the Tarim Basin. In: Tang, X. G. and Liang, D. G. (Eds), Paper Compilation of Oil and Gas Formation in the Tarim Basin. Xinjiang Science and Sanitation Press, (Wulumuqi), pp. 545-551 (in Chinese).

TONG, X. G., 1991. The tectonics and hydrocarbon accumulation in the Tarim Basin. In: Tang, X. G. and Liang, D. G. (Eds), Paper Compilation of Oil and Gas Formation in the Tarim Basin. Xinjiang Science and Sanitation Press, (Wulumuqi), pp. 321-330 (in Chinese).

WANG, Q. and LI, H., 1993. Data base of Tarim Petroleum Geology and Geochemistry. Internal Report. Tarim Petroleum Institute. pp. 1-324 (in Chinese).

XIAO, X.M., 1997. Organic petrology and hydrocarbon potentials of Triassic dark mudstone in the Tarim Basin. *Geochemistry* **26** (1), 64-71 (in Chinese).

XIAO, X.M., LIU, D.H. and FU, J.M., 2000a. Dating hydrocarbon generation and migration by means of bitumen reflectance. *Chinese Science Bulletin* **45** (19), 2123-2127(in Chinese).

XIAO, X.M., LIU, Z.F., and LIU, D.H., 2000b. A new method to reconstruct hydrocarbon – generating histories of source rocks in a petroleum bearing basin – a method of geological and geochemical sections. *Chinese Science Bulletin* **45** (supplement issue), 97-104.

XIAO, X.M., FU, J.M. and Liu, D.H., 1991. The possibility of reflectance of amorphinite (micrinite) as a mature level parameter of source rocks, *Progress in National Science* **1** (4), 357-361.

XIAO, X.M., (Ed.). 1992. Organic petrology and Its application to oil and gas exploration. Guangdong Scientific Press. Guangzhou. pp 70-108 (in Chinese).

XIAO, X.M., WILKINS, R.W.T., LIU, D.H. *et al.*, 2000c. Investigation of thermal maturity of lower Palaeozoic hydrocarbon source rocks by means of vitrinite-like maceral reflectance. *Organic Geochemistry* **31**(11), 1041-1052.

XIAO, X.M., LIU, Z.F. and SHENG, J.Q., 1998. Characterization and origin types of immature and low-mature amorphous kerogen in terrestrial source rocks. *Chinese Sciences Bulletin* **43** (3), 241-244.

XIAO, X.M., LIU, D.H. and SHEN, J.Q., 2001. Study of geochemistry of oil and gas pools in the Lunnan Area, Tarim Basin. An Internal Report. Guangzhou Institute of Geochemistry, Chinese Academy of Sciences, Guanhzhou, 76-89 (in Chinese).

YUNG, T.S. and LIU, W.C., 1991. Palaeogeographic evolution and sedimentary history in Palaeozoic age in the Tarim Basin. In: Tang, X. G. and Liang, D. G (Eds), Paper Compilation of Oil and Gas Formation in the Tarim Basin. Xinjiang Science and Sanitation Press, (Wulumuqi), pp.103-116 (in Chinese).

ZHANG, S.C., HANSON, A.D., MOLDOWAN, J.M., *et al.*, 2000. Paleozoic oil-source rock correlations in the Tarim basin, NW China. *Organic Geochemistry* **31**, 273-286.

ZHUO, X.J., TAN, M. and QIOU, Y.Y., 1997. Discussion on the structural types and models for oil and gas pools. *Experimental Petroleum Geology*, **19** (2), 148-157 (in Chinese).

ZHOU, G.X., HUANG, H.W. and SI, C., 1991. Types of oil and gas pools and their geological characteristics in the Taibei Uplift, Tarim Basin. In: Tang, X.G. and Liang, D.G. (Eds), Paper Compilation of Oil and Gas Formation in the Tarim Basin. Xinjiang Science and Sanitation Press, (Wulumuqi), pp. 574-588 (in Chinese).